

# Regional Specialization of the Membrane of Retinal Glial Cells and Its Importance to $K^+$ Spatial Buffering<sup>a</sup>

ERIC A. NEWMAN

*Eye Research Institute of Retina Foundation  
Boston, Massachusetts 02114*

The regulation of extracellular  $K^+$  levels,  $[K^+]_o$ , in the central nervous system (CNS) is essential for the maintenance of neuronal function. Spatial buffering by glial cells is believed to play an important role in this process.<sup>1,2</sup> As suggested originally by Orkand, Nicholls, and Kuffler,<sup>3</sup> excess  $K^+$  deposited into interstitial space as a result of neuronal activity will enter  $K^+$ -permeable cells in regions of raised  $[K^+]_o$ . In order to maintain net electrical neutrality, an equal amount of  $K^+$  will exit from these cells, or from cells electrically coupled to them, in regions where  $[K^+]_o$  is lower. The effect of this  $K^+$ -mediated current flow is to transfer  $K^+$  from regions where  $[K^+]_o$  is high to regions where  $[K^+]_o$  is low.

Astrocytes, which are almost exclusively permeable to  $K^{+4,5}$  and which form large syncytia of cells coupled together by low-resistance gap junctions,<sup>6,7</sup> are thought to mediate  $K^+$  spatial buffering in the brain. In the vertebrate retina, astrocytes are relatively sparse. Instead, the principal glial element is the Müller cell, a specialized radial glial cell that resembles astrocytes in many respects.<sup>8</sup>

Müller cells extend from the inner (vitreal) surface of the retina to the outer limiting membrane (at the level of the photoreceptor inner segments).<sup>8</sup> The membrane properties of these cells make them ideally suited to regulate  $[K^+]_o$  in the retina through the process of  $K^+$  spatial buffering. As I will demonstrate below, the membrane conductance of Müller cells is highly selective for  $K^+$ . This  $K^+$  conductance is not distributed uniformly over the cell surface, but rather is concentrated in specific regions of the cell. This nonuniform conductance distribution serves to greatly enhance the effectiveness of  $K^+$  spatial buffering in the retina. Furthermore, Müller cells possess voltage-dependent ion channels that may also function to amplify spatial buffering currents.

## $K^+$ SELECTIVITY OF MÜLLER CELLS

The efficiency of  $K^+$  spatial buffering is limited by the ion selectivity of the cells carrying the spatial buffering current. If cells are exclusively permeable to  $K^+$ , then

<sup>a</sup>This research was supported by National Institutes of Health Grant EY 04077.

the  $K^+$  influx that occurs at the site of a  $[K^+]_o$  increase will be matched by an equal  $K^+$  efflux in other regions. If, however, the cell is also permeable to  $Cl^-$  or to cations other than  $K^+$ , the  $K^+$  influx will be partially neutralized by currents carried by these other ions. The  $K^+$  efflux needed to balance the current will be smaller and less  $K^+$  will be transferred by the spatial buffering process.

I have measured the  $K^+$  selectivity of Müller cells in a series of ion-substitution experiments made on retinal slices of the frog.<sup>9</sup> Cells were penetrated in their cell bodies, in the inner nuclear layer. As shown in FIGURE 1 (filled circles), Müller cells depolarized when  $K^+$  of the perfusate was raised. The cell membrane potential ( $E_m$ ) closely followed the  $K^+$  equilibrium potential (FIG. 1, straight line) over a wide range, deviating only when  $K^+$  of the perfusate was below 2.5 mM.

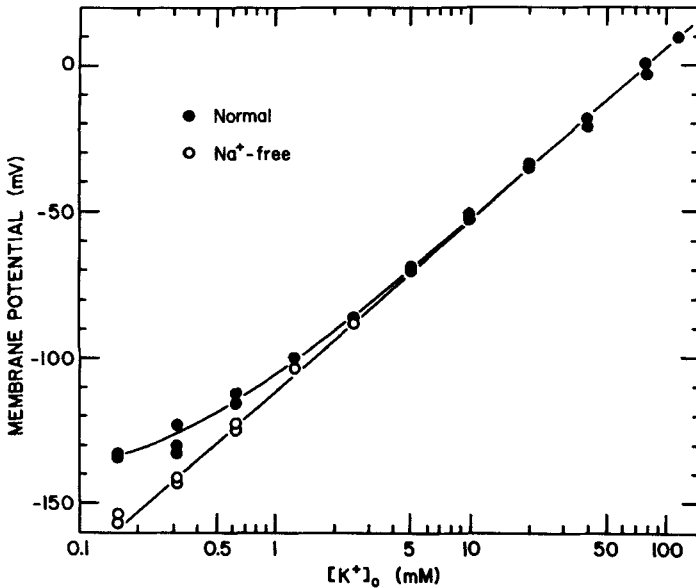


FIGURE 1. Müller cell membrane potential as a function of perfusate  $[K^+]$ . All data from a single cell recorded from a frog retinal slice. The cell is almost exclusively permeable to  $K^+$ . In normal perfusate (filled circles)  $E_m$  deviates from the  $K^+$  equilibrium potential (straight line) only when  $[K^+]$  is lower than 2.5 mM. In Na-free perfusate (open circles),  $E_m$  follows  $E_K$  faithfully. (From Newman<sup>9</sup> with permission from *Journal of Neuroscience*.)

The ion selectivity of the Müller cell membrane can be estimated by fitting the data points in FIGURE 1 by the Goldman equation, incorporating both  $K^+$  and  $Na^+$  permeabilities. An excellent fit was obtained (FIG. 1, curved line) when a  $K^+ : Na^+$  permeability ratio of 490 : 1 was assumed.<sup>9</sup> That the deviation of  $E_m$  from the  $K^+$  equilibrium potential was due to a small  $Na^+$  conductance was confirmed in a second series of ion-substitution experiments. When  $Na^+$  was omitted from the perfusate, Müller cell  $E_m$  followed the  $K^+$  equilibrium potential, even at low  $[K^+]$  (FIG. 1, open circles). In other experiments,<sup>9</sup> Müller cell  $E_m$  remained constant when  $[Cl^-]$  was reduced from 91 to 8 mM, demonstrating that the cell was largely impermeable to

$\text{Cl}^-$  as well. Taken together, these experiments demonstrate that Müller cells are almost exclusively permeable to  $\text{K}^+$ .

## NONUNIFORM $\text{K}^+$ CONDUCTANCE DISTRIBUTION OVER THE CELL SURFACE

Experiments conducted during the past decade have suggested that the  $\text{K}^+$  conductance of Müller cells is not distributed uniformly over the cell surface. Current source-density analysis of the b-wave of the electroretinogram (ERG)<sup>10,11</sup> indicated that light-evoked current efflux from Müller cells was restricted to the cell's endfoot, a Müller cell process lying at the inner border of the retina. This suggested that a large fraction of the cell's  $\text{K}^+$  conductance was localized in the endfoot process.<sup>10</sup> A similar suggestion was offered by Tomita and his colleagues based on their studies of field potentials generated during spreading depression episodes<sup>12,13</sup> and by intraretinal injections of  $\text{K}^+$ .<sup>14,15</sup>

### *Input Impedance Measurements*

The hypothesis that there is a nonuniform distribution of  $\text{K}^+$  conductance across the Müller cell surface has been tested in a number of ways using intracellular recordings from *in situ* and dissociated amphibian Müller cells. The most direct test of the hypothesis has come from input-impedance measurements on dissociated salamander Müller cells.

If a large fraction of the  $\text{K}^+$  conductance of the Müller cell is localized in the endfoot process, then the input resistance of the cell should rise significantly if this portion of the cell is removed. This was accomplished experimentally by a simple microdissection procedure. When the stalk process of a dissociated salamander Müller cell is cut with a glass needle (FIG. 2), the two cut ends of the stalk often reseal, leaving viable cell bodies without endfeet and isolated endfoot processes.

The input impedance of single dissociated cells was monitored in recordings made from the cell body region.<sup>9,16</sup> As illustrated in FIGURE 3 (A and B), both the input resistance and time constant of the cell increased approximately 20-fold when the endfoot process was removed during the microdissection procedure. Cell resistance increased from a mean value of 7.9 Mohm to 152 Mohm following endfoot removal (No. = 24). This indicates that 95% of the total membrane conductance of the cell resides in or near the endfoot process.

It could be argued that the increase in cell resistance does not reflect the true distribution of membrane conductance over the cell surface, but rather is caused by mechanical disruption of the cell membrane, or perhaps by a change in the ionic composition of the cell cytoplasm. This possibility was tested by measuring the input impedance of isolated endfoot processes prepared by the same microdissection procedure used to remove the endfoot from the remainder of the cell.

Recordings made from the endfoot showed that, in contrast to the cell body, input resistance did not increase very much when the cell stalk was cut<sup>9,16</sup> (FIG. 3D). (The resistance increased from 8 to 15 Mohm, but most of this increase was due to damage

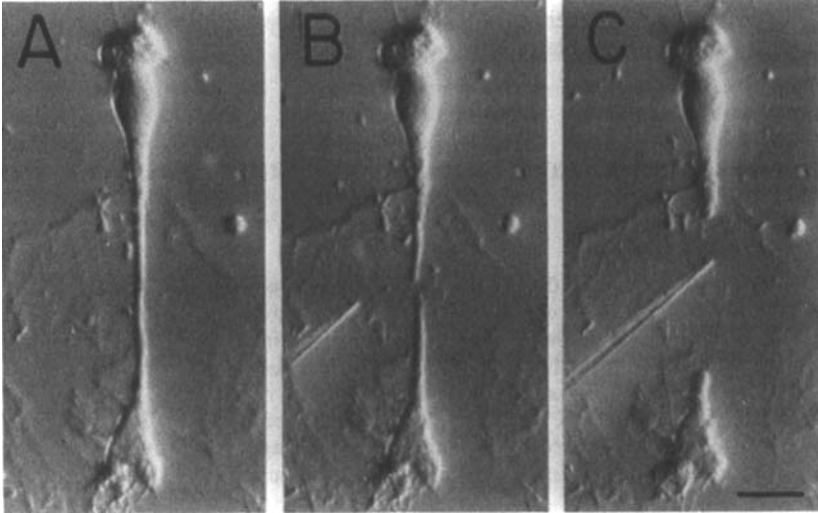


**FIGURE 2.** Photomicrographs of a dissociated salamander Müller cell microdissected with a glass needle. (A) Intact cell. (B) 15 seconds after the stalk was cut. (C) Several minutes later. This microdissection procedure was employed in order to measure the input impedance of each half of the cell independently. Scale bar, 20  $\mu\text{m}$ . (From Newman<sup>9</sup> with permission from *Journal of Neuroscience*.)

to the endfoot membrane.) In addition, the membrane time constant of isolated endfeet was much shorter than that of the intact cell (0.17 versus 0.7 msec; compare FIG. 3D with 3C), indicating that the endfoot membrane had a larger specific conductance than the remainder of the cell.

### *K<sup>+</sup> Ejection Responses*

The nonuniform distribution of conductance across the surface of Müller cells was confirmed in a second series of experiments where responses of dissociated salamander cells to localized increases in  $[\text{K}^+]_o$  were monitored.<sup>9,16</sup> Müller cell  $E_m$  was recorded from the cell body while focal  $[\text{K}^+]_o$  increases were generated by pressure-ejecting a 125 mM KCl solution from an extracellular pipette positioned against the surface of the cell.

FIGURE 4 shows a series of  $\text{K}^+$  responses recorded from a dissociated Müller cell. When  $\text{K}^+$  was ejected at the proximal face of the endfoot, a large depolarization was recorded (FIG. 4, trace a). When the ejection pipette was moved to the lateral face of the endfoot (FIG. 4, trace b; a distance of only 8  $\mu\text{m}$ ) the response was decreased sevenfold.  $\text{K}^+$  ejections to the stalk, cell body, and apical end of the cell (FIG. 4, traces c, d, and f) produced responses only 1.4 to 3.7% the proximal endfoot response; however,  $\text{K}^+$  ejected at the neck of the cell (FIG. 4, trace e) produced a response 5 to 13 times larger than ejections to neighboring regions.

What do these responses tell us about the distribution of conductance across the

Müller cell surface? It can be shown, using an ohmic model of the Müller cell, that the amplitude of cell responses to focal  $K^+$  ejections is directly proportional to the  $K^+$  conductance of that portion of the Müller cell membrane experiencing the  $[K^+]$  increase,<sup>9</sup> thus, the  $K^+$  ejection results confirm that the endfoot process of the cell has a much larger  $K^+$  conductance than do other cell regions. In addition, the results demonstrate that this high conductance is localized primarily to the proximal face of the endfoot, that portion of the cell that is directly apposed to the vitreous humor *in vivo* (compare FIG. 4, traces a and b). Quantitatively, the results indicate that the specific conductance of different regions of the cell, relative to the proximal endfoot, are as follows: proximal face of endfoot, 100%; lateral face of endfoot, 18.4%; stalk, 1.8%; cell body, 1.6%; neck, 13.0%; apical end, 2.1% (No. = 21).

A similar series of  $K^+$  ejection experiments were conducted on Müller cells *in situ* in retinal slices of the salamander and frog.<sup>9</sup> Intracellular recordings were made from Müller cells penetrated in the inner nuclear layer of slices while a 100 mM KCl solution was ejected into specific retinal layers. Qualitatively, the responses recorded from retinal slices confirmed those obtained from dissociated cells.  $K^+$  ejections into the nerve fiber layer, that is, onto the endfoot membrane, produced larger cell depolarizations than did  $K^+$  ejections in other retinal layers. In addition, in some cells,  $K^+$  ejections in the outer plexiform layer (the location of the "neck" of the cell) produced larger responses than did ejections into adjacent retinal layers. Quantitative estimates of specific membrane conductance could not be obtained from retinal slice experiments, however, because the dynamics of the spread of  $K^+$  from the ejection site to the Müller cell surface were not known.

### NONUNIFORM $K^+$ CONDUCTANCE DISTRIBUTION AND SPATIAL BUFFERING

The experiments described above provide convincing evidence that a large fraction of the total  $K^+$  conductance of Müller cells is confined to the endfoot process. This

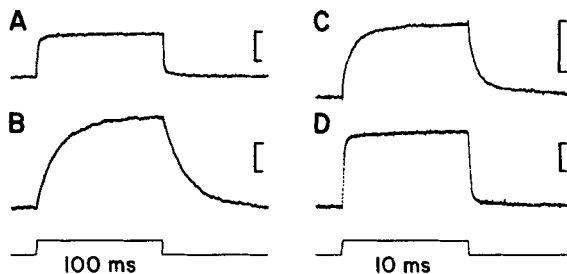


**FIGURE 3.** Input impedance measurements of dissociated salamander Müller cells. (A) Response of an intact cell to a 1-nA current pulse. (B) Response of the same cell to a 0.1-nA pulse following removal of the endfoot process. The cell input resistance and time constant both increased approximately 21-fold. (C) Response of an intact cell to a 1-nA pulse, shown at a faster sweep speed. (D) Response of an isolated endfoot process to a 1-nA pulse. Input resistance rose moderately while the time constant decreased. Scale bars, 5 mV. (From Newman<sup>9</sup> with permission of *Journal of Neuroscience*.)

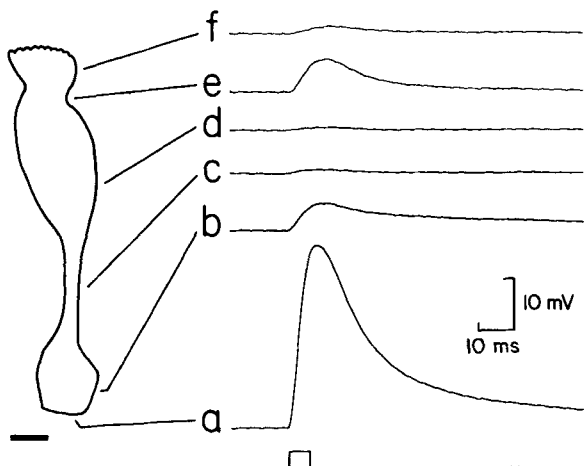


**FIGURE 4.** Responses to focal  $K^+$  ejections recorded from the cell body of a dissociated salamander Müller cell (shown schematically at left). Ejections were directed at: a, proximal face of the endfoot (inner limiting membrane); b, lateral face of the endfoot (nerve fiber layer); c, stalk (inner plexiform layer); d, cell body (inner nuclear layer); e, neck (outer plexiform layer); f, apical end of the cell (rod inner segment layer). Based on these responses, the specific  $K^+$  conductance of the proximal face of the endfoot of this cell was estimated to be 81 times larger than that of the cell body. The neck conductance was approximately 13 times larger than the cell body conductance. Scale bar for drawing of cell, 10  $\mu\text{m}$ .

nonuniform distribution of  $K^+$  conductance has important implications for the regulation of interstitial  $K^+$  levels by Müller cells. If  $K^+$  conductance were distributed uniformly over the cell surface, spatial buffering by Müller cells would function to redistribute a localized  $[K^+]_o$  increase across the entire thickness of the retina. This is illustrated in FIGURE 5A, which indicates the pattern of  $K^+$  fluxes across the Müller cell membrane (arrows) following a  $[K^+]_o$  increase in the inner plexiform layer. In this situation, the local  $[K^+]_o$  increase is attenuated, but only at the expense of raising  $[K^+]_o$  in other retinal layers.

Because  $K^+$  conductance is principally localized in the endfoot process of Müller cells, the actual pattern of spatial buffering currents will be quite different. As illustrated in FIGURE 5B, almost all of the  $K^+$  current entering the Müller cell from the site of  $[K^+]_o$  increase will leave the cell at the proximal face of the endfoot. This  $K^+$  will, in turn, diffuse directly into the vitreous humor, which will act as a nearly infinite  $K^+$  sink. This modified form of spatial buffering, which has been termed " $K^+$  siphoning,"<sup>17</sup> has a distinct advantage over the traditionally envisaged form of  $K^+$  buffering: excess  $K^+$ , instead of being transferred to neighboring regions of neural tissue, is deposited in the vitreous, where it will not influence retinal activity. Because 95% of the conductance of Müller cells is localized to the endfoot process, 95% of all  $K^+$  transferred by Müller cell spatial buffering will leave the cell via the endfoot.

$K^+$  siphoning by Müller cells is a powerful mechanism for removing excess  $K^+$  from the retina. It occurs, however, at a cost. In order to achieve a high-endfoot  $K^+$  conductance relative to the remainder of the cell, the absolute conductance of most of the cell is low (0.14  $\text{mS}/\text{cm}^2$  versus 31  $\text{mS}/\text{cm}^2$  for the endfoot<sup>9</sup>). Computer simulations demonstrate that this low specific conductance is the limiting factor in

the amount of  $K^+$  that can be transferred by  $K^+$  siphoning.<sup>17,18</sup> If the conductance of the main body of the cell were higher, more  $K^+$  would be transferred by  $K^+$  currents, but a smaller percentage of the  $K^+$  would be directed into the vitreous.

The nonuniform distribution of  $K^+$  conductance along the length of the cell body of Müller cells may help to counter the effects of the low average conductance of this region of the cell. The  $K^+$  ejection experiments described above demonstrate that the specific conductance of the Müller cell membrane that lies within the outer plexiform layer (the neck of dissociated cells) is six to eight times larger than the conductance of the cell in neighboring retinal layers. The outer plexiform layer is one of the two retinal laminae where light-evoked  $K^+$  increases occur.<sup>19</sup> Thus, the conductance of the Müller cell membrane is larger in precisely that region where influx of  $K^+$  current takes place. This specialization of the Müller cell membrane offsets the low average conductance of the cell body and will increase the effectiveness of  $K^+$  siphoning several-fold.

### EXPERIMENTAL DEMONSTRATION OF $K^+$ SIPHONING

The process of  $K^+$  siphoning, which was originally proposed because the endfeet of Müller cells were found to have high  $K^+$  conductance, has been demonstrated experimentally.<sup>17</sup> The apical end of dissociated salamander Müller cells were exposed to increased  $[K^+]_o$  by ejection of a 100 mM KCl solution from an extracellular pipette. Efflux of  $K^+$  from other regions of the cell was then monitored using a  $K^+$ -selective micropipette (FIG. 6A). Responses of the  $K^+$  electrode are shown in FIGURE 6B. A large  $[K^+]_o$  increase was recorded when the ion-selective pipette was positioned at the

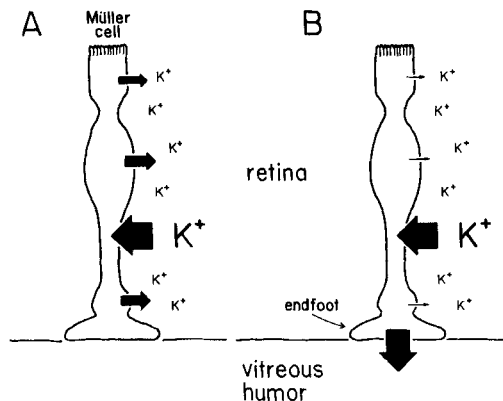


**FIGURE 5.** Diagrams illustrating the process of  $K^+$  siphoning by Müller cells in the retina. (A) If  $K^+$  conductance was distributed uniformly over the cell surface, an increase in  $[K^+]_o$  in the inner plexiform layer would cause a  $K^+$  influx into Müller cells in this region (large arrow) and a  $K^+$  efflux from all other regions of the cell (small arrows). (B) Because most of the conductance of the Müller cell is localized to the endfoot process, almost all  $K^+$  efflux will occur from this region. Excess  $K^+$  from the inner plexiform layer will be transferred to the vitreous humor rather than to other retinal layers, as in A.

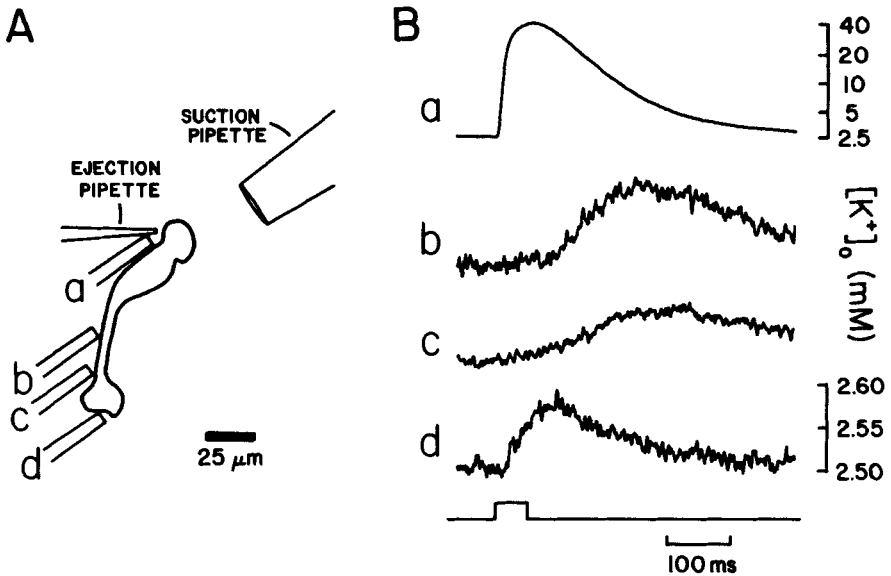


**FIGURE 6.** Experimental demonstration of  $K^+$  siphoning. (A) The apical end of a dissociated salamander Müller cell was exposed to increased  $[K^+]_o$  by ejecting an 85 mM KCl solution from an ejection pipette. Efflux of  $K^+$  from other regions of the cell was monitored with a  $K^+$ -selective micropipette (a through d). (B) Responses recorded from the  $K^+$ -selective electrode.  $K^+$  efflux from the cell was only detected at site d, the proximal face of the endfoot. Traces b, c, and d are expanded vertically relative to trace a. (From Newman *et al.*<sup>17</sup> with permission from *Science*.)

site of  $K^+$  ejection (FIG. 6B,a). Much smaller  $[K^+]_o$  increases were measured when the  $K^+$  electrode was moved to the stalk of the cell (FIG. 6B, b and c). These increases were generated by diffusion and bulk flow of  $K^+$  from the ejection site, as indicated by their slower time courses and the decrease in their amplitude with distance.

When the  $K^+$  electrode was positioned against the proximal face of the endfoot (FIG. 6B, d), the slow  $[K^+]_o$  rise was absent but was replaced by a rapid, transient increase. This  $[K^+]_o$  increase, which had latencies as short as 4 msec in many cases, was due to  $K^+$  efflux from the endfoot membrane. These results demonstrate that when  $K^+$  enters a Müller cell at the site of a  $[K^+]_o$  increase,  $K^+$  exits from the cell primarily from the endfoot process. This is precisely what is expected given the distribution of  $K^+$  conductance across the surface of the Müller cell membrane.

## VOLTAGE-DEPENDENT ION CHANNELS

Recent experiments<sup>20</sup> have demonstrated that, in addition to the voltage-independent  $K^+$  conductance of the endfoot, Müller cells possess four types of voltage-dependent ion channels: a  $Ca^{2+}$  channel, a  $Ca^{2+}$ -activated  $K^+$  channel, a fast-inactivating (type A)  $K^+$  channel and an inward-rectifying  $K^+$  channel. (The voltage-dependent  $Ca^{2+}$  channel generates electrically activated " $Ca^{2+}$  spikes" when the resting



$K^+$  conductance of Müller cells is blocked.<sup>20</sup>) These four channels have been characterized in voltage-clamp studies on dissociated salamander Müller cells.<sup>20</sup> As illustrated by their current-voltage (*I-V*) relationships (FIG. 7), three of these channels (the  $Ca^{2+}$  channel, the  $Ca^{2+}$ -activated  $K^+$  channel and the type-A  $K^+$  channel) open only when the cell is depolarized to  $-60$  mV or less; however, the fourth type of channel, the  $K^+$  inward rectifier, undergoes large conductance changes near the cell resting level.

The  $K^+$  inward rectifying channel is probably of the most importance functionally, as it is the only voltage-dependent channel that is open under physiological conditions. The properties of this channel are complex (see FIG. 7B). Channel conductance is

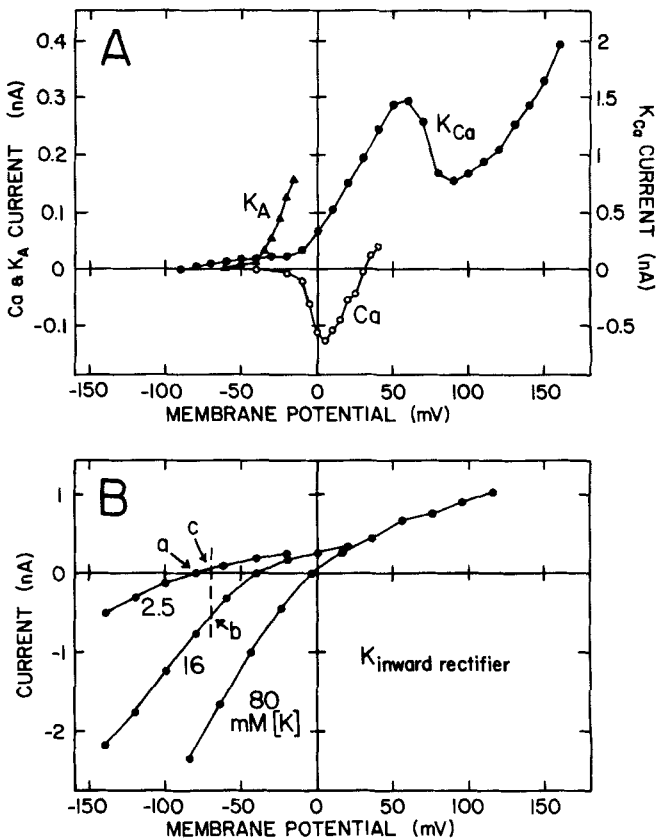


**FIGURE 7.** Current-voltage relations of four voltage-dependent currents recorded from dissociated salamander Müller cells. These plots were obtained from whole-cell voltage clamp experiments using single, patch electrodes. (A) Inward  $Ca^{2+}$  currents (Ca) and outward  $Ca^{2+}$ -activated  $K^+$  currents ( $K_{Ca}$ ) were observed when cells were depolarized to greater than  $-40$  mV. Type A  $K^+$  currents ( $K_A$ ) were observed for depolarizations to greater than  $-60$  mV. (B) Inward rectifier  $K^+$  currents were recorded from a cell bathed sequentially in 2.5, 16, and 80 mM  $K^+$  perfusate. The dashed line and points a-c in (B) are included to illustrate changes in channel conductance due to a localized  $[K^+]_o$  increase. See text for details. (From Newman.<sup>20</sup>)

significantly larger when the cell is hyperpolarized than when it is depolarized. In addition, the entire I-V relation of the channel shifts to the right when  $[K^+]_o$  is raised.

The influence that inward-rectifying  $K^+$  channels have on  $K^+$  spatial buffering can be appreciated by considering their properties. If  $[K^+]_o$  is raised from 2.5 to 16 mM over a restricted region of the cell surface, for example, the I-V relation of those channels exposed to the  $K^+$  increase will be shifted to the right (FIG. 7B, curve "16" versus curve "2.5"). The  $[K^+]_o$  increase will depolarize the cell moderately, to a level indicated by the dashed vertical line in FIG. 7B; the high conductance of the Müller cell endfoot has the effect of shunting the membrane potential to near the resting level, even for large focal increases in  $[K^+]_o$  (see Newman<sup>9</sup>). The conductance of the channels exposed to 16 mM  $K^+$  (given by the slope of the I-V curve at point b in FIG. 7B), is 4.2 times larger than the conductance at rest (the slope at point a, FIG. 7B).

At the same time, the I-V relation of those channels not exposed to the  $[K^+]_o$  increase remains unchanged (FIG. 7B, curve "2.5"). The conductance of these channels will be smaller (by 20%) than at rest, however, because the cell is partially depolarized by the  $[K^+]_o$  increase (compare the slope of the I-V curve at c with the slope at a, FIG. 7B). It should be borne in mind that, under physiological conditions, the changes in inward-rectifying conductance will probably be less dramatic than those illustrated here, as light-evoked increases in retinal  $[K^+]_o$  probably do not reach 16 mM.<sup>21-23</sup>

The example illustrated above suggests that inward-rectifying  $K^+$  channels enhance the process of  $K^+$  spatial buffering in two ways. First, the  $K^+$  and voltage-dependent properties of the channel lead to an increased membrane conductance in regions exposed to  $[K^+]_o$  increase. This, in turn, results in a greater influx of  $K^+$  into Müller cells. Secondly, the voltage-dependent properties of the channel lead to a reduction in the membrane conductance in other regions of the cell, reducing the amount of  $K^+$  that is deposited in neighboring regions of retinal tissue. (Efflux of  $K^+$  from the endfoot process will not be reduced by cell depolarization as it occurs through  $K^+$  channels that are largely voltage-independent; E. A. Newman, unpublished observations.)

## $K^+$ SIPHONING IN THE BRAIN

Müller cells are a specialized form of radial glial cell that share many properties with astrocytes and radial glia in the brain.<sup>8,24</sup> The endfeet of astrocytes and Müller cells are homologous. Both terminate on basal laminae. Müller cell endfeet lie against the inner limiting membrane next to the vitreous humor while the endfeet of astrocytes lie against capillaries and the pial surface of the brain. In both types of cells, high densities of orthogonal arrays of intramembranous particles (assemblies) are found on those membrane surfaces apposed to the basal laminae.<sup>25,26</sup>

It would not be surprising then, to find that the endfeet of astrocytes and radial glial cells in the brain, like those of Müller cells, possess high  $K^+$  conductance. Such a membrane specialization would serve an important role in brain  $K^+$  homeostasis.  $K^+$  spatial buffering currents entering glial cells in regions of increased  $[K^+]_o$  would be shunted out through their endfoot processes, directly into the blood plasma or the cerebrospinal fluid. In the absence of an endfoot specialization, on the other hand, excess  $K^+$  would be deposited into neighboring neural tissue; thus, the directed flow of spatial buffering currents through the endfoot processes, that is,  $K^+$  siphoning,

would play an important role in enhancing the process of  $K^+$  spatial buffering in the brain, as it does in the retina.

*K<sup>+</sup> Conductance Distribution in Astrocytes*

Recent experiments from my laboratory<sup>27</sup> suggest that the endfoot processes of astrocytes do, in fact, have high  $K^+$  conductance. The experiments were performed on freshly dissociated astrocytes of the optic nerve of salamander (*Ambystoma*),

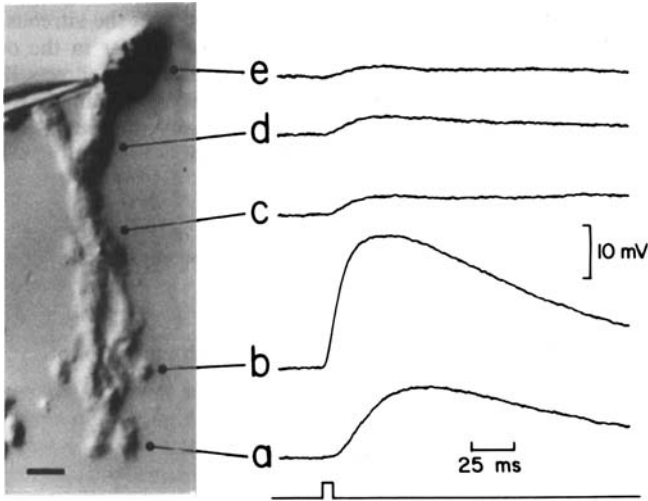


**FIGURE 8.** Responses of a dissociated astrocyte from the optic nerve of salamander to focal  $K^+$  ejections. A photograph of the cell (with recording electrode attached) is shown at left.  $K^+$  ejections directed at two of the endfeet of the cell (a and b) produced significantly larger cell depolarizations than did ejections directed at the main process of the cell (c and d) and the cell soma (e). These results demonstrate that, as in Müller cells, the endfeet of astrocytes have significantly greater  $K^+$  conductance than other regions of the cell. Scale bar for photograph, 10  $\mu$ m.

prepared by the same enzymatic digestion procedure used to isolate Müller cells.<sup>9</sup> As illustrated in FIGURE 8, the cells isolated from the optic nerve had one to several stout processes radiating from a large cell body. The processes often branched into finer extensions that ended in terminal enlargements. These cells were electrically inexcitable in control perfusate and were judged to be astrocytes; astrocytes are the primary, if not only, type of cell found in the optic nerve of salamanders.<sup>28</sup>

The distribution of  $K^+$  conductance across the surface of these cells was tested by monitoring cell responses to focal  $K^+$  ejections. Responses evoked by ejections directed at astrocyte endfeet were significantly larger than were responses to ejections in other cell regions. This is illustrated in FIGURE 8, where the  $K^+$  responses of two

of the endfeet of an astrocyte (traces a and b) were 3 to 11 times larger than were the responses of the main process of the cell (traces c and d) and the cell body (trace e). These results demonstrate that, as in Müller cells, a large fraction of the  $K^+$  conductance of astrocytes is localized in their endfeet.

## SUMMARY

Electrophysiological experiments, obtained primarily from dissociated salamander cells, demonstrate that the  $K^+$  conductance of Müller cells is distributed in a highly nonuniform manner over the cell surface. A large fraction of the total cell conductance is localized to that portion of the endfoot process that faces the vitreous humor. Along the remainder of the cell, specific  $K^+$  conductance is larger in the outer plexiform layer than in neighboring regions. High-endfoot conductance directs  $K^+$  spatial buffering currents preferentially through the endfoot process, leading to an efficient form of spatial buffering termed  $K^+$  siphoning. Preliminary experiments suggest that the endfeet of astrocytes also have high  $K^+$  conductance.

## ACKNOWLEDGMENTS

I thank Janice I. Gepner for her comments on the manuscript.

## REFERENCES

1. DIETZEL, I., U. HEINEMANN, G. HOFMEIER & H. D. LUX. 1980. Transient changes in the size of the extracellular space in the sensorimotor cortex of cats in relation to stimulus-induced changes in potassium concentration. *Exp. Brain Res.* **40**: 432-439.
2. GARDNER-MEDWIN, A. R. 1983. Analysis of potassium dynamics in mammalian brain tissue. *J. Physiol.* **335**: 393-426.
3. ORKAND, R. K., J. G. NICHOLLS & S. W. KUFFLER. 1966. The effect of nerve impulses on the membrane potential of glial cells in the central nervous system of amphibia. *J. Neurophysiol.* **29**: 788-806.
4. ORKAND, R. K. 1977. Glial Cells. *In Handbook of Physiology*. Sec. 1, vol. 1, part 2. pp. 855-875. American Physiological Society. Bethesda, Md.
5. WALZ, W., W. WUTTKE & L. HERTZ. 1984. Astrocytes in primary culture: Membrane potential characteristics reveal exclusive potassium conductance and potassium accumulator properties. *Brain Res.* **292**: 367-374.
6. BRIGHTMAN, M. W. & T. S. REESE. 1969. Junctions between intimately apposed cell membranes in the vertebrate brain. *J. Cell Biol.* **40**: 648-677.
7. GUTNICK, M. J., B. W. CONNERS & B. R. RANSOM. 1981. Dye-coupling between glial cells in the guinea pig neocortical slice. *Brain Res.* **213**: 486-492.
8. NEWMAN, E. A. 1986. The Müller cell. *In Astrocytes*. S. Fedoroff & A. Vernadakis, Eds. Academic Press. (In press.)
9. NEWMAN, E. A. 1985. Membrane physiology of retinal glial (Müller) cells. *J. Neurosci.* **5**: 2225-2239.
10. NEWMAN, E. A. 1979. b-Wave currents in the frog retina. *Vision Res.* **19**: 227-234.

11. NEWMAN, E. A. 1980. Current source-density analysis of the b-wave of frog retina. *J. Neurophysiol.* **43**: 1355-1366.
  12. MORI, S., W. H. MILLER & T. TOMITA. 1976. Müller cell function during spreading depression in frog retina. *Proc. Natl. Acad. Sci. USA* **73**: 1351-1354.
  13. MORI, S., W. H. MILLER & T. TOMITA. 1976. Microelectrode study of spreading depression (SD) in frog retina—Müller cell activity and  $K^+$  during SD. *Jpn. J. Physiol.* **26**: 219-233.
  14. FUGIMOTO, M. & T. TOMITA. 1981. Field potentials induced by ejection of potassium ion into the frog retina: A test of current interpretations of the electroretinographic (ERG) b-wave. *Brain Res.* **204**: 51-64.
  15. YANAGIDA, T. & T. TOMITA. 1982. Local potassium concentration changes in the retina and the electroretinographic (ERG) b-wave. *Brain Res.* **237**: 479-483.
  16. NEWMAN, E. A. 1984. Regional specialization of retinal glial cell membrane. *Nature* **309**: 155-157.
  17. NEWMAN, E. A., D. A. FRAMBACH & L. L. ODETTE. 1984. Control of extracellular potassium levels by retinal glial cell  $K^+$  siphoning. *Science* **225**: 1174-1175.
  18. BREW, H. & D. ATWELL. 1985. Is the potassium channel distribution in glial cells optimal for spatial buffering of potassium? *Biophys. J.* **48**: 843-847.
  19. KARWOSKI, C. J., E. A. NEWMAN, H. SHIMAZAKI & L. M. PROENZA. 1985. Light-evoked increases in extracellular  $K^+$  in the plexiform layers of amphibian retinas. *J. Gen. Physiol.* **86**: 189-213.
  20. NEWMAN, E. A. 1985. Voltage-dependent calcium and potassium channels in retinal glial cells. *Nature* **317**: 809-811.
  21. KARWOSKI, C. J. & L. M. PROENZA. 1977. Relationship between Müller cell responses, a local transretinal potential and potassium flux. *J. Neurophysiol.* **40**: 244-259.
  22. KLINE, R. P., H. RIPPS & J. E. DOWLING. 1978. The generation of b-wave currents in the skate retina. *Proc. Natl. Acad. Sci. USA* **75**: 5727-5731.
  23. DICK, E. & R. F. MILLER. 1985. Extracellular  $K^+$  activity changes related to electroretinogram components. I. Amphibian (I-type) retinas. *J. Gen. Physiol.* **85**: 885-909.
  24. VARON, S. S. & G. G. SOMJEN. 1979. Neuron-glia interactions. *Neurosci. Res. Prog. Bull.* **17**(1).
  25. RAVIOLA, G. 1977. The structural basis of the blood-ocular barriers. *Exp. Eye Res.* **25**(S): 27-63.
  26. LANDIS, D. M. D. & T. S. REESE. 1974. Arrays of particles in freeze-fractured astrocytic membranes. *J. Cell Biol.* **60**: 316-320.
  27. NEWMAN, E. A. 1986. High potassium conductance in astrocyte end feet. *Science* **233**: 453-454.
  28. BRACHO, H., P. M. ORKAND & R. K. ORKAND. 1975. A further study of the fine structure and membrane properties of neuroglia in the optic nerve of *Necturus*. *J. Neurobiol.* **6**: 395-410.
- 

### DISCUSSION

E. E. NATTIE (*Dartmouth Medical School, Hanover, NH*): How does the potassium cycle back into the plexiform cells?

E. A. NEWMAN (*Eye Research Institute of Retina Foundation, Boston, MA*): One of the main questions regarding the mechanism of potassium movement into the vitreous or into the blood or the CSF is: How do you get it back? I am assuming a completely passive model, and when potassium levels in the retina or the brain are reduced again by uptake of  $K^+$  into neurons, then the system will work in reverse,

and it will behave symmetrically so that potassium can flow back into the retina or the brain.

N. J. ABBOTT (*King's College, London*): This comment relates to invertebrates. If the blood-brain barrier is actually formed by glial cells in many of these invertebrates so that the glial cells line the blood vessel, then your potassium would move directly into the blood. In animals where the endothelium forms the barrier and glial endfeet terminate there, it actually gives you better control, I think, because you can dump potassium into this glial region or space between glia and barrier that is in contact with CSF. Then you wouldn't necessarily lose all that potassium into the blood so you could get it back again quickly after a transient rise. So there may be some merit in separating the barrier from the glial process.

NEWMAN: But in case of glia at the level of the capillaries this space, if there is any, would be relatively small. This region couldn't function as a good storage site for potassium. So if there's any siphoning to this region, it would have to be pumped into the capillary, or it would quickly be saturated.

ABBOTT: There's quite good evidence that this space, although small, is in continuity with the CSF and the subarachnoid spaces.

C. NICHOLSON: As you know, in many lower vertebrates, lizards and turtles for example, the principal type of glia seems to be long ependymal cells that span the distance between the surface membranes of the brain and the ventricles. They are sometimes a millimeter long, which is five times the length of the Müller cell and often very fine in geometry. Do you think that these cells have enough capacity to carry potassium over long distances?

NEWMAN: If these radial glial cells have the very fine processes that they appear to have, then I don't think that influx into these processes in the middle of a brain would make its way out to the extremities. I think the space constant of the cell would be too short, and it would not work efficiently. There would have to be other potassium transport mechanisms in that case.

A. R. GARDNER-MEDWIN (*University College London, London, England*): The nonlinear properties of the membrane channel that we're talking about, the inward rectifier, are particularly useful in buffering. Can you give us any data about the voltage level at which this channel is turned on and where you think it would be relevant; in changing light levels, for example?

NEWMAN: I've made one estimate of the change in conductance. If you have an increase in extracellular potassium from 2.5 mM to 16 mM, which is not quite physiological, the conductance of the membrane exposed to the potassium increase will be 4.2 times greater than the conductance of the region not exposed, so it's a very significant change in potassium conductance. It certainly will be smaller than that in the retina because potassium doesn't go up to 16 mM, but it will be significant. The inward rectifier I-V curve has its greatest change in slope centered at the resting potential of the cell, so that for any excursion in the membrane potential or changes in potassium, you get a change in conductance.